Early apatite deposition and osteoblast growth on plasma-sprayed dicalcium silicate coating

Xuanyong Liu,[1,2] Youtao Xie,[1,2] Chuanxian Ding,[1] Paul K. Chu[2]
[1]*Shanghai Institute of Ceramics, Chinese Academy of Sciences, 1295 Dingxi Road, Shanghai 200050, China*
[2]*Department of Physics and Materials Science, City University of Hong Kong, Tat Chee Avenue, Kowloon, Hong Kong*

Received 23 April 2004; revised 4 November 2004; accepted 4 November 2004
Published online 11 July 2005 in Wiley InterScience (www.interscience.wiley.com). DOI: 10.1002/jbm.a.30273

Abstract: Dicalcium silicate coating was deposited onto a Ti-6Al-4V substrate using plasma-spraying technology. The coating was immersed in simulated body fluid (SBF) for 1, 3, 6, 12, 24, and 48 h to investigate early apatite formation on the coating. Osteoblasts were also seeded onto the surface of the dicalcium silicate coating to evaluate its biocompatibility. Cold field-emission scanning electron microscopy and energy-dispersive X-ray spectrometry were used to evaluate the morphologies and determine the chemical composition of the coatings. The surface structural changes caused by immersion in SBF were analyzed using thin-film X-ray diffraction. After the dicalcium silicate coating was soaked in SBF solution 1–6 h, two types of particles containing calcium and phosphorus were formed on the surface. One type consisted of relatively larger particles (P1) precipitated on the surface of the coating from the precursor cluster formed in the SBF solution. The second type was composed of particles (P2) nucleated on the surface of the coating. With increasing immersion time, the particles coalesced to form a surface Ca-P layer. The Ca-P layer was composed of amorphous calcium phosphate that was not transformed to crystalline apatite until the immersion time in SBF exceeded 24 h. The formation mechanism of the Ca-P layer and apatite on the surface of the coating is believed to be involved in the formation of the Si 3-ring active surface site with negative charge. The cell-seeding test revealed that osteoblasts grew and proliferated very well on the surface of the dicalcium silicate coating. © 2005 Wiley Periodicals, Inc. J Biomed Mater Res 74A: 356–365, 2005

Key words: dicalcium silicate; plasma spraying; apatite; osteoblast

INTRODUCTION

Since Hench et al.[1] discovered a group of special glasses based on the 45S5 Bioglass® to bond with bone, many kinds of $CaO \cdot SiO_2$-based glasses and ceramics have been developed to adhere directly to bone tissues. Kokubo[2] and Ohtsuki et al.[3] showed that the $CaO\text{-}SiO_2$ components contributed mainly to the bioactivity of the $CaO \cdot SiO_2$-based glass and ceramics. De Aza et al.[4] pointed out that wollastonite ceramics ($CaSiO_3$) were bioactive. Nonami and Tsutsumi,[5] working with diopside ($CaO\text{-}MgO\text{-}2SiO_2$) ceramics, found that an apatite layer was formed on the surface of diopside ceramics implanted into the bones of rabbits and monkeys. In our previous work, it was also found that carbonate-containing hydroxyapatite was formed on the surface of plasma-sprayed wollastonite coatings after being soaked in the simulated body fluid (SBF) for a certain time,[6] indicating that the materials have excellent bioactivity.

The bioactivity of plasma-sprayed dicalcium silicate (Ca_2SiO_4) coating was also investigated in our previous work.[7] An obvious apatite top layer and a silica-rich interlayer were observed on the surface of the coating soaked in SBF for 2 days, as shown Figure 1. There are several articles addressing apatite crystal nucleation and growth, and different mechanisms have been proposed to explain apatite nucleation on the surface of the $CaO\text{-}SiO_2$-based bioceramics.[8–10] The precise mechanisms by which surfaces promote heterogeneous apatite precipitation are not known because of the difficulty in char-

Correspondence to: P. K. Chu; e-mail: paul.chu@cityu.edu.hk

Contract grant sponsor: Shanghai Science and Technology R&D Fund; contract grant numbers: 02QE14052, 03JC14074
Contract grant sponsor: Hong Kong Research Grants Council (RGC) Competitive Earmarked Research Grant (CERG); contract grant number: CityU1137/03E
Contract grant sponsor: National Natural Science Foundation of China (NSFC) and Hong Kong Research Grants Council (RGC) Joint Research Scheme; contract grant number: N_CityU101/03
Contract grant sponsor: Germany/Hong Kong Joint Research Scheme sponsored by the Hong Kong RGC and German Academic Exchange Service; contract grant number: G_HK001/02

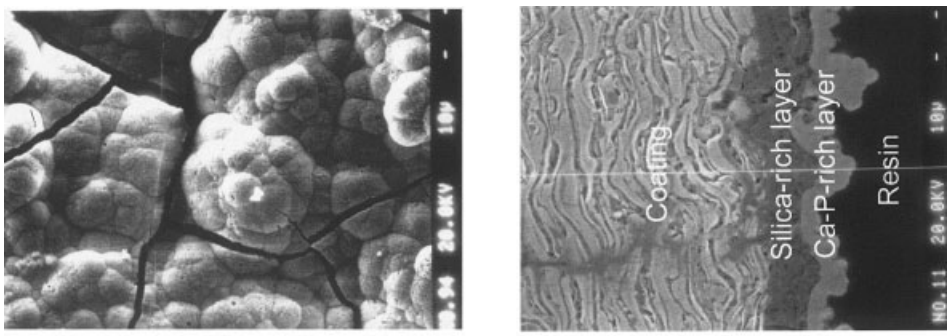

Figure 1. (a) Surface and (b) cross-section views of the dicalcium silicate coating soaked in SBF after 48 h.

acterizing the earliest angstrom- or nanometer-sized solid precipitates. Fortunately, the advent of field-emission scanning electron microscopy (FE-SEM) has made it easier to observe and investigate nano-sized particles. In this work, the mechanism of apatite formation on dicalcium silicate coating was investigated by observing the early deposition of apatite (first 2 days) on the surface of the coating while being soaking in SBF.

Osteoblasts constitute the cell type responsible for the deposition of bone within the interface between an implant and host tissue and have a fundamental role in the successful clinical outcome of orthopedic/dental prostheses. Bagambisa and Joos[11] stated that the osteomorphogenesis was closely associated with the phenomenological behavior of cells (anchorage, attachment, adhesion, and spreading). With regard to the determination of biochemical and molecular biological parameters, the cell morphology is an important feature.[12] Therefore, cellular morphology is an accepted parameter in biocompatibility tests. In this work, the morphologies of bone-derived rat osteoblasts after culture on the surface of a plasma-sprayed dicalcium silicate coating were determined in order to evaluate the biocompatibility of the coating.

MATERIALS AND METHODS

SBF soaking test

Dicalcium silicate (Ca_2SiO_4) powders were synthesized in our laboratory. The typical size of the powders was approximately 5–30 μm. An atmospheric plasma spraying system (Sulzer Metco, Switzerland) was used to fabricate dicalcium silicate coatings onto Ti-6Al-4V substrates with dimensions of 10 × 10 × 2 mm for both the SBF soaking and osteoblast culturing tests.

After being ultrasonically washed in acetone and rinsed in deionized water, the specimens were soaked in the SBF solution for 1, 3, 6, 12, 24, and 48 h at 36.5°C without stirring. The ion concentrations of the SBF solution are nearly equal to those of the human body blood plasma. The SBF solution was buffered at pH 7.4 with trimethanol aminomethane-HCl.

A JEOL JSM-6700F cold FE-SEM and an energy-dispersive X-ray (EDS) detector were used to determine the morphologies and the elemental composition of the coatings after immersion. Surface structural changes of the coating after immersion in SBF were analyzed by thin-film X-ray diffraction (XRD). The XRD experiments were performed at a glancing angle of 2° to improve the surface sensitivity. The changes in the concentrations of calcium, silicon, and phosphorus in the SBF solution due to the immersion of specimens were measured by inductively coupled plasma atomic emission spectroscopy.

Osteoblast seeding test

Osteoblasts were obtained from the calvaria of 20-day-old fetal rats. After excising the calvaria aseptically, the endo- and extracranial periostea were mechanically removed. The calvaria were kept in Hanks buffer at 4°C and then incubated for 2 × 10 min in a phosphate-buffered saline (PBS) solution (plus 4 n*M* ethylenediaminetetraacetic acid) and rinsed for 3 × 5 min with PBS. A preincubation step using collagenase (1 mg/mL PBS, 10 min at 37°C) was conducted to remove periosteal fibroblasts and cell debris, and the supernatant was discarded. After a continuous enzyme treatment (2 × 30 min), the resulting supernatants were centrifuged (5 min at 1400 rpm). The pellet obtained was resuspended in a culture medium: α-minimum essential medium containing 5% inactivated fetal calf serum, 1 mg/mL glucose, and 90 μg/mL gentamicin. The sterile specimens were each placed in six-well culture dishes and then seeded at a cell density of approximately 2×10^4 cells/mL in the complete culture medium containing sodium ascorbate (50 μg/mL) and β-glycerolphosphate (10 m*M*). On every sample, 200 μL of a cell suspension was applied with great care and the cells were allowed to attach for 2 h to the underlying substrate, and then 3.5 mL of the culture medium was carefully added.

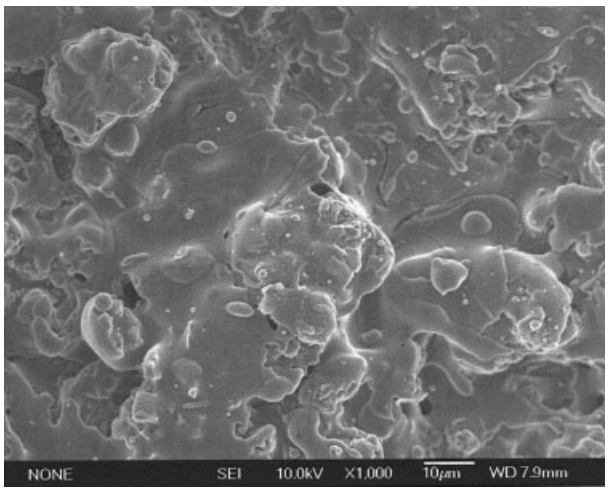

Figure 2. Surface views of the as-sprayed dicalcium silicate coating.

After 4-, 7-, and 12-day cultures, samples were fixed in 2.5% glutaraldehyde in 0.1*M* sodium cacodylate buffer (pH = 7.4) for 1 h, rinsed with PBS (3 × 10 min), and dehydrated in a grade ethanol series. Critical point drying of the samples was followed by gold sputtering. The samples were examined at 10 kV using FE-SEM.

RESULTS

The changes of the surface morphology of the dicalcium coatings with immersion time (1–24 h) in SBF were investigated to examine the formation of apatite on the surface of the coating.

The surface views of the as-sprayed dicalcium silicate coating reveal that the coating has a rough surface with some protuberances and some relatively flat areas (Fig. 2). After soaking in SBF for 1 h, some particles (denoted by P1) appear on the coating surface, as shown in Figure 3(a,b). The EDS spectrum of the particle discloses the presence of calcium, silicon, and phosphorus [Fig. 3(c)], whereas the corresponding EDS spectra acquired from the area without particles [labeled A in Fig. 3(b)] reveal only silicon and calcium

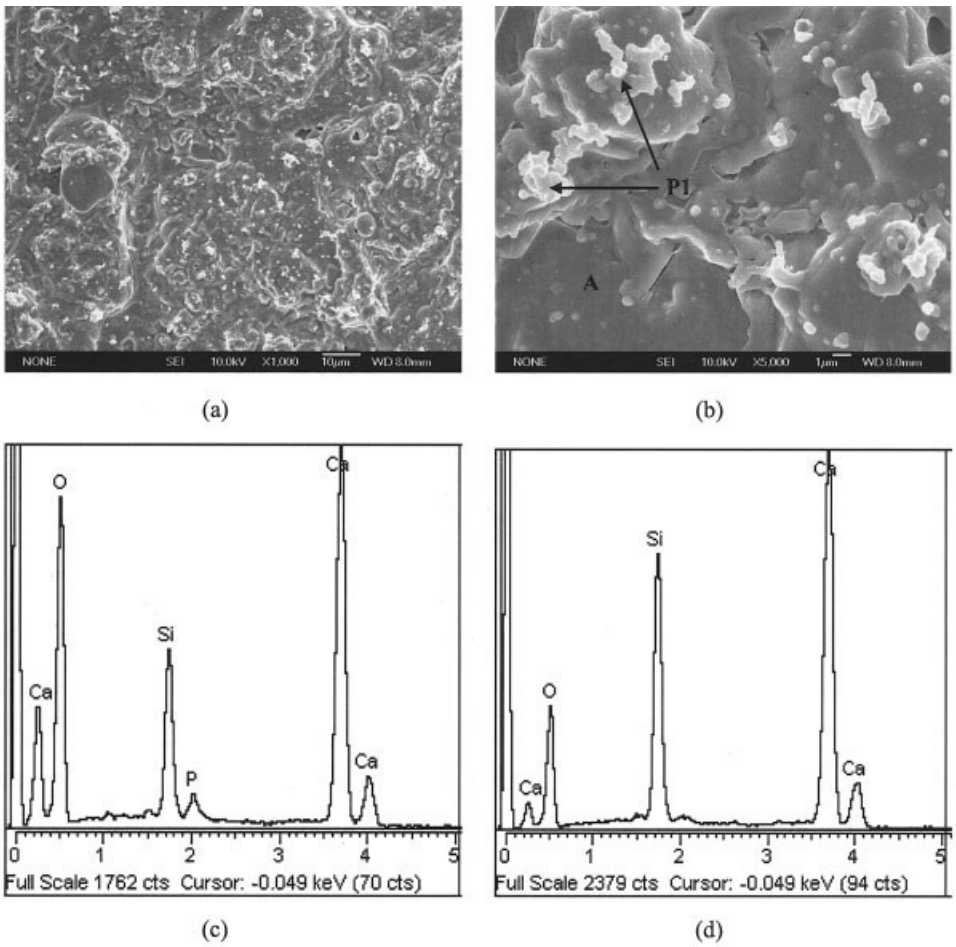

Figure 3. Surface views and EDS spectra acquired from the dicalcium silicate coating soaked in SBF after 1 h: (a) original magnification 1000×, (b) original magnification 5000×, (c) EDS spectrum taken from the P1 particles, and (d) EDS spectrum taken from area A in (b).

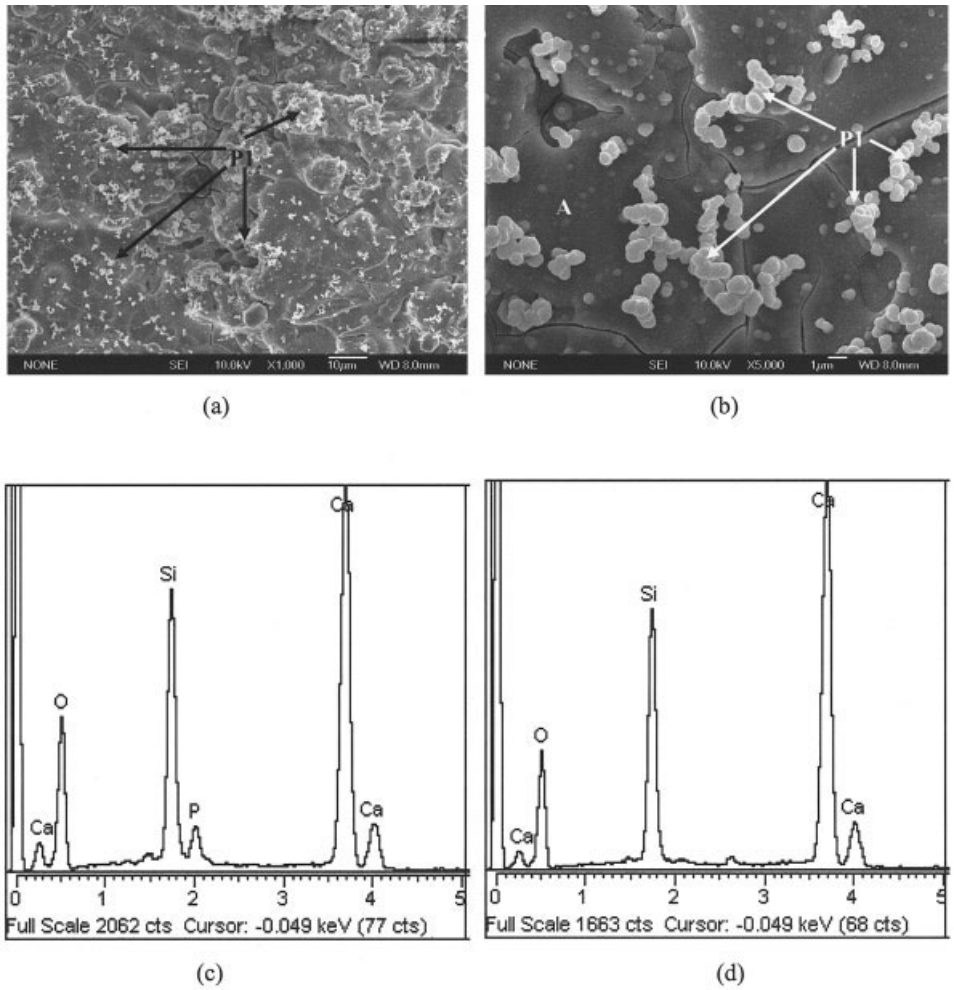

Figure 4. Surface views and EDS spectra of the dicalcium silicate coating soaked in SBF after 3 h: (a) original magnification 1000×, (b) original magnification 5000×, (c) EDS spectrum acquired from the P1 particles, and (d) EDS spectrum taken from area A in (b).

[Fig. 3(d)]. The results indicate that that the particles are composed of clusters containing phosphate, whereas there is no detectable phosphate in the other areas.

With longer immersion time in the SBF solution (up to 3 h), more particles (denoted by P1) appear on the surface of the coating [Fig. 4(a,b)]. The particles are larger than those on the coating after 1 h. The EDS spectrum taken from the particle reveals that the relative intensity of the phosphorus peak increases slightly with increasing immersion time from 1 to 3 h [Fig. 4(c)], indicating a higher phosphate content in the particles. Phosphorus cannot yet be detected in the area without particles [labeled A in Fig. 4(b)], as shown in Figure 4(d). Some microcracks can be found on the surface of the coating. The microcracks are produced from the drying process due to the shrinking of the newly formed silica-rich layer from the reaction between the coating and SBF solution.

After soaking in SBF for 6 h, many particles (P1) emerge on the surface of the coating, as shown in Figure 5(a). The higher-magnification micrograph reveals that many small column-like particles about 100 nm in size are incorporated into the P1 particles [Fig. 5(b)]. At the same time, we can find similar column-like particles (denoted by P2) nucleating in other areas [labeled A in Fig. 5(b)]. The EDS spectrum of the area A confirms that the P2 particles are also composed of the clusters containing phosphorus [Fig. 5(d)].

When the immersion time in SBF reaches 12 h, the surface is covered by a new layer composed of particles about 100 nm in size [Fig. 6(a,b)]. More phosphorus can be detected by EDS [Fig. 6(c)].

The surface views and EDS spectrum of the dicalcium coating soaked in SBF solution for 24 h show that the surface is now covered completely by the Ca-P layer, as shown in Figure 7. Only calcium and phosphorus and no silicon are detected on the coating by EDS indicating that the Ca-P layer has achieved a significant thickness. The higher-magnification view discloses that the Ca-P layer comprises many small particles about 100 nm in size.

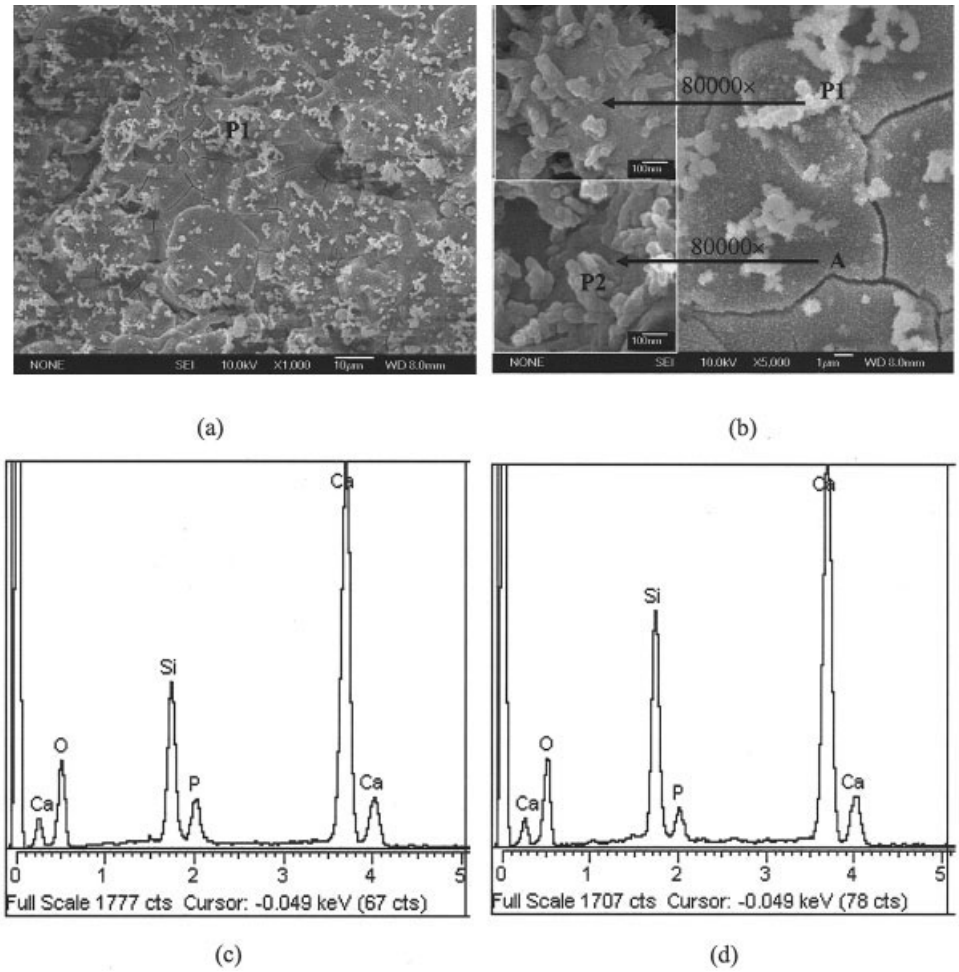

Figure 5. Surface views and EDS spectra of the dicalcium silicate coating soaked in SBF after 6 h: (a) original magnification 1000×, (b) original magnification 5000×, (c) EDS spectrum obtained from the P1 particles, and (d) EDS spectrum taken from area A in (b).

In summary, after the dicalcium silicate coating has been soaked in SBF solution 1–6 h, two types of phosphorus-containing particles form on the coating. One of them consists of relatively large particles (P1) precipitated on the coating from the solution when the immersion time in SBF is 1 h. After longer immersion time in SBF, these particles become more abundant and higher-magnification micrographs show that they are in fact made up of many small particles. The EDS spectrum reveals the presence of silicon, calcium, and phosphorus in the particles. A second type of particle (P2) is found to nucleate on the surface of the dicalcium coating after a longer soaking time of 6 h. When the immersion time reaches 24 h, the surface of the dicalcium silicate coating is completely covered by the Ca-P layer that is so thick that silicon in the substrate can no longer be detected by EDS.

The XRD spectra of the as-sprayed dicalcium silicate coating and the coatings soaked in SBF for 1, 3, 6, 12, 24, and 48 h are depicted in Figure 8. The XRD pattern of the as-sprayed dicalcium coatings shows that the crystalline phase of the coating is mainly β-Ca_2SiO_4. The primary peak of the crystalline β-Ca_2SiO_4 is at $2\theta = 32.556°$, corresponding to the (200) crystal plane (JSPDS 24-0037). The primary peak of the crystalline apatite is at $2\theta = 31.795°$, corresponding to the (211) crystal plane (JSPDS 34-0010). The particles containing calcium and phosphorus emerge on the surface of the coating soaked in SBF solution 1, 3, and 6 h, and an obvious Ca-P layer is observed on the surface of the dicalcium silicate coating soaked in SBF for 12 h, but crystalline apatite cannot yet be detected by XRD. This may be because the calcium- and phosphorus-containing particles and Ca-P layer are still composed of amorphous calcium phosphate and have not crystallized to form apatite. It is well known that the calcium phosphate phase which accumulates on the surface of CaO-SiO_2-based glasses and glass-ceramics is initially amorphous. It later crystallizes to a carbonate-containing hydroxyapatite structure by incorporating carbonate anions from the solution within the amorphous calcium phosphate phase.[8] With long immersion time

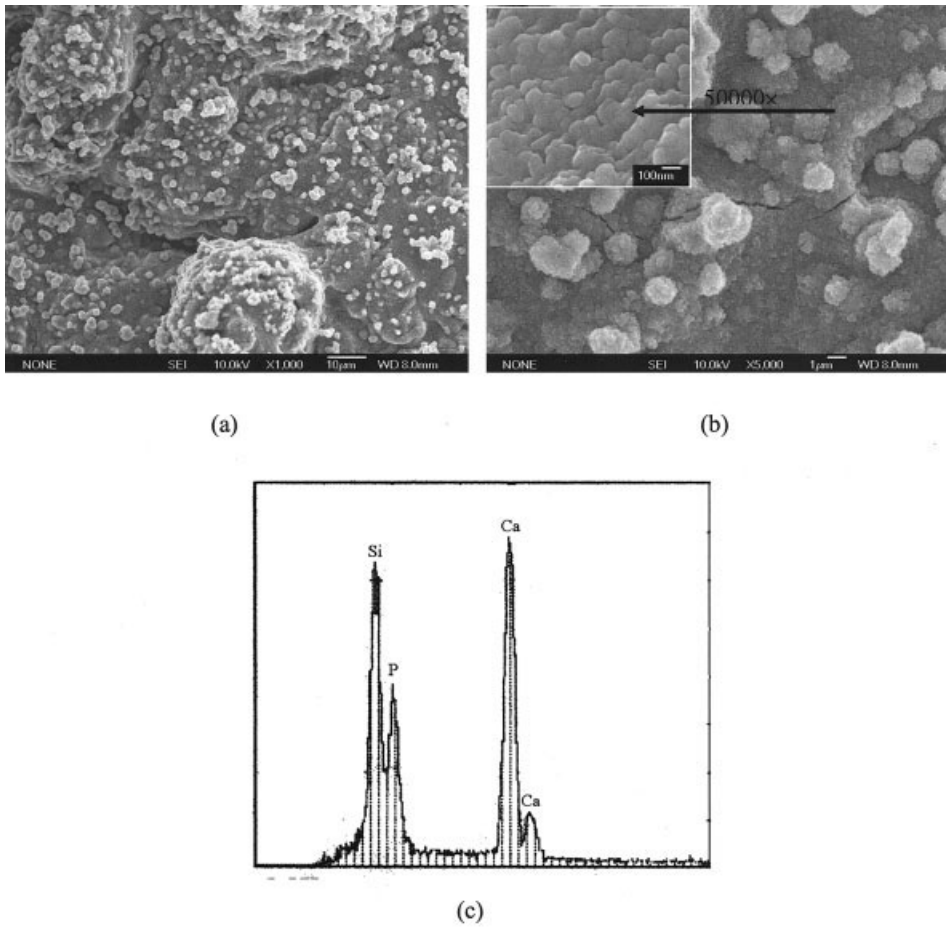

Figure 6. Surface views and EDS spectra of the dicalcium silicate coating soaked in SBF after 12 h: (a) original magnification 1000×, (b) original magnification 5000×, and (c) EDS spectrum corresponding to the whole area in (a).

in SBF (up to 24 h), the peaks of the crystalline β-Ca_2SiO_4 disappear gradually. In addition, some characteristics of apatite begin to emerge in the XRD spectra. The primary peak at around $2\theta = 32°$ is split into two peaks, one corresponding to β-Ca_2SiO_4 and the other to apatite. More peaks corresponding to the crystalline apatite appear in the XRD spectrum when the immersion time increases to 48 h, indicating the formation of more crystalline apatite on the dicalcium silicate coating.

Changes in the concentration of the calcium, silicon, and phosphorus as well as the pH of the SBF solution with immersion time are shown in Table I. It can be seen that the concentration of calcium and silicon as well as pH of the SBF solution increase with longer immersion time. The ionic exchanges between H^+ within SBF solution and Ca^{2+} in the coating result in the increase in the pH and the concentration of the calcium ion of the SBF solution. The higher silicon concentration is a result of the formation of soluble silicon caused by the ion exchange between the coating and the SBF solution. The phosphorus concentration in the SBF solution decreases gradually with longer immersion time due to the precipitation of the phosphorus-containing clusters.

Figure 9 exhibits the views of osteoblasts seeded on the surface of the dicalcium silicate coating after different times. Osteoblasts are observed to grow and proliferate very well on the coating surface. After 4 days, the surface of the dicalcium silicate coating is covered completely by the cells and extracellular matrix. The cell shows a good morphology with many dorsal ruffles and filopodia. With longer seeding time, the cells fuse to form a complete layer on the coating surface.

DISCUSSION

According to Sahai and Tossell,[13] at the near-neutral pH range of blood plasma, the planar Si 3-ring is the active surface site on silica bioceramics. Calcium ions adsorb as an inner-sphere complex to the negatively charged surface site followed by HPO_4^{2-}, resulting in an acidic, hydrated, precursor cluster with 2–3 U of

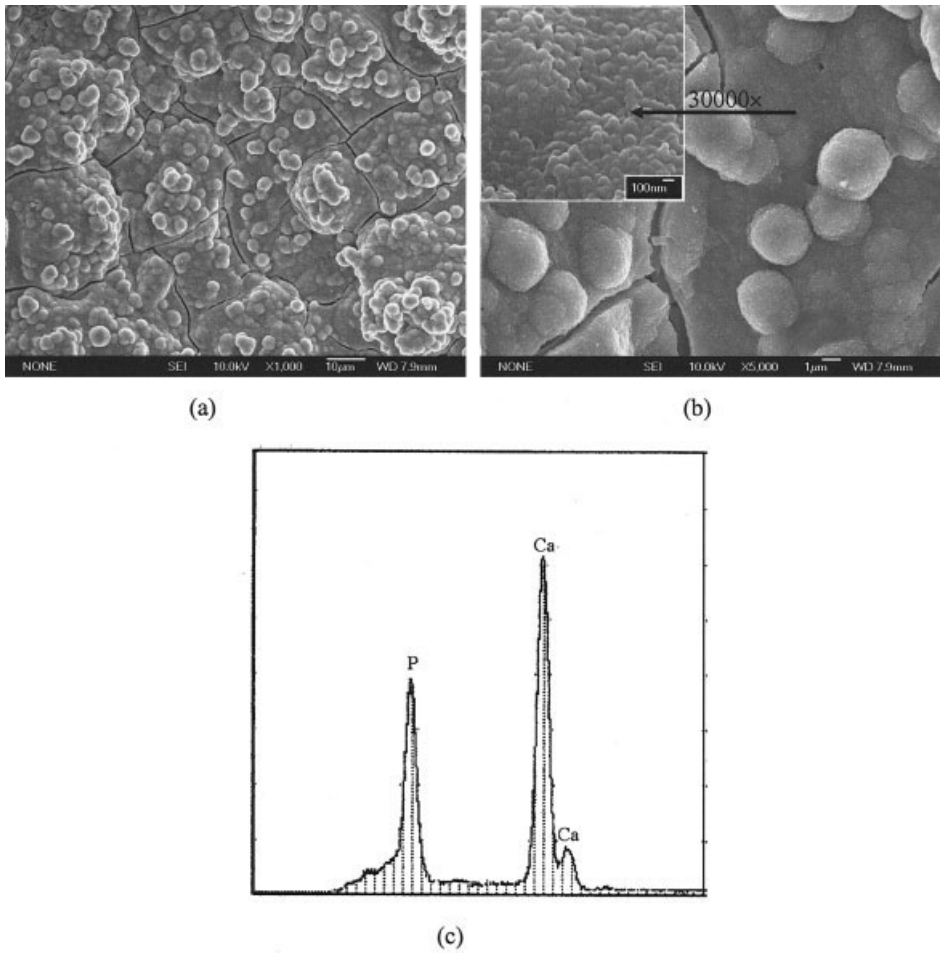

Figure 7. Surface views and EDS spectra of the dicalcium silicate coating soaked in SBF after 24 h: (a) original magnification 1000×, (b) original magnification 5000×, and (c) EDS spectrum corresponding to the whole area in (a).

calcium hydrogen phosphate. The predicted precursor is a surface complex or surface oligomer, not a well-defined mineral phase. After the initial nucleation of the acidic precursor surface oligomer, the mechanism is thought to involve aggregation and growth of oligomers by H-bonds with subsequent transformation to crystalline apatite. The pathway of apatite formation on the surface of the silica bioceramics is as follows:

$$\text{Silica bioceramics} \rightarrow [Si_3O_6H_5^-] \rightarrow [Si_3O_6H_5Ca(H_2O)_6]^+ \rightarrow [Si_3O_6H_5CaHPO_4(H_2O)_3]^- \rightarrow \text{Apatite}$$

Dicalcium silicate is an isolated silicate without bridging oxygen atoms. Some reports[14] indicate that orthosilicates hydrolyze more rapidly than other silicate species (e.g., disilicate, chain silicate) because the bridging oxygen is much more resistant to attack than nonbridging oxygen. Hence, the presence of the orthosilicate species will promote an easier leaching by exchanging H_3O^+ ions from the solution with alkaline earth ions concentrated in the orthosilicate positions, which will lead to the formation of a silica-rich layer on the surface of the coating. At the same time, soluble silicon also dissolves into the solution.

Therefore, the formation of apatite on the surface of the dicalcium silicate coating soaked in SBF can be postulated as follows. Calcium ions in the coating initially exchange with H_3O^+ in the SBF solution leading to the formation of a silica-rich layer on the coating accompanied by the dissolution of silicon into the SBF solution. The soluble silicon in the SBF solution polymerizes to form the Si 3-ring. Calcium ions adsorb as an inner-sphere complex onto the negatively charged surface site followed by HPO_4^{2-}, resulting in an acidic, hydrated, precursor cluster with 2–3 U of calcium hydrogen phosphate. Then, once the precursor cluster becomes sufficiently larger, it will precipitate onto the surface of the coating, corresponding to the P1 particles depicted as above. The point of zero charge (pH_{pzc}) for silica is at pH ≈ 3–4,[15] which means that above this pH, the silica surface has a net negative charge. The magnitude of the negative charge increases with increasing pH. When the immersion time in SBF is up to 6 h, the Si 3-ring active surface site with

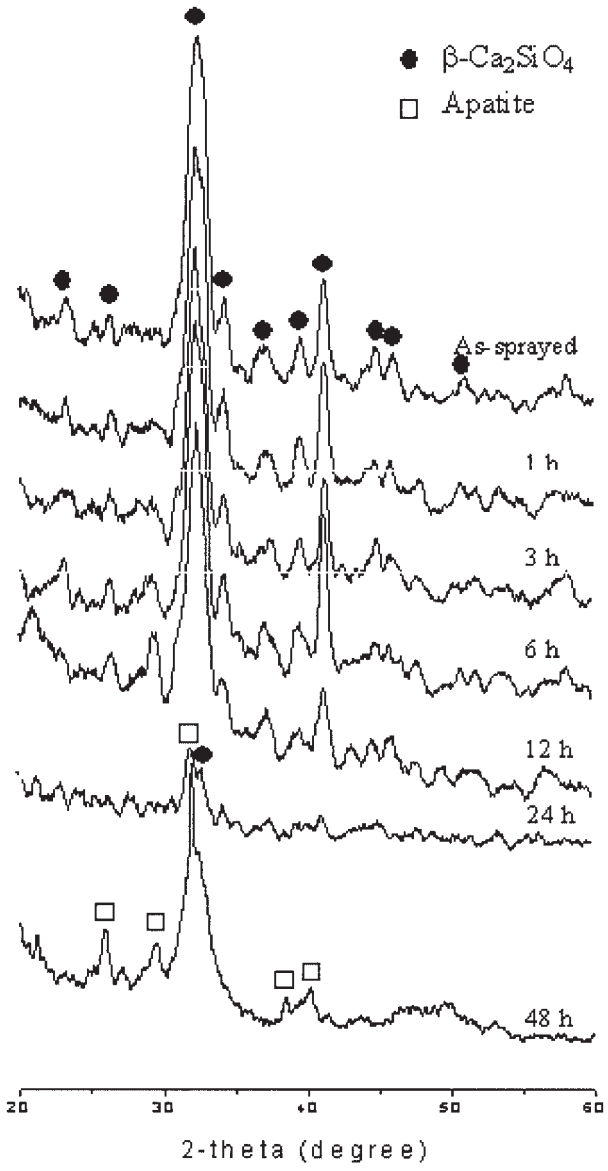

Figure 8. XRD spectra acquired from the dicalcium silicate coating soaked in SBF for different periods of time.

negative charge also forms on the silica-rich layer, and then the precursor cluster containing calcium and phosphorus nucleates on the surface to form the P2 particle. After longer immersion time, the precursor clusters aggregate, grow, and subsequently transform to crystalline apatite.

Osteoblasts are observed in our experiments to grow and proliferate very well on the surface of the dicalcium silicate coating as well. The reason may be attributed to the nature of the underlying substrate and the local chemical environment which is suitable for the proliferation of osteoblasts due to the dissolution of the coatings. The dissolution products from the dicalcium silicate coating in the body fluid are composed of hydrated silicon and calcium ions. Hildebrand et al.[16] and Hench[17] have used modern genetic engineering techniques to demonstrate that certain genes are activated by hydrated silicon. Hydrated soluble silicon will enhance the proliferation of bone cells (osteoblasts) and active cellular production of transforming growth factors.[17,18] Xynos et al.[19,20] have also shown that the critical concentration of ionic products dissolved from the bioactive glass composed of soluble silicon and calcium ions can enhance osteogenesis through a direct control over the genes that regulate cell cycle induction and progression. In addition, the process of cell spreading is also influenced by the nature of the underlying substrate. Some studies have indicated that the appearance of the bioactive layer containing highly negative-charged groups and creating a high local pH ($7 < pH < 9$) certainly influences the behavior and morphology of the osteoblasts cultured an the bioactive coatings.[21] Our experiments indicate that dicalcium silicate coating possesses excellent biocompatibility.

CONCLUSION

After the dicalcium silicate coating has been soaked in SBF solution from 1 to 6 h, two types of calcium- and phosphorus-containing particles form on the surface of the coating. One of them comprises relatively large particles (P1) precipitated on the surface of the coating from the precursor cluster formed in the SBF solution. Another type consists of particles (P2) nucleated on the surface of the coating. With increasing immersion time, the particles aggregate and grow to form a Ca-P layer on the surface of the coating. The Ca-P layer is still composed of amorphous calcium phosphate and has not transformed to crystalline apatite until the immersion time in SBF exceeds 24 h. The formation mechanism of the Ca-P layer and apatite on the surface of the coating is believed to be involved in the forma-

TABLE I
Elemental Concentration and pH of the SBF Before and After Soaking the Dicalcium Silicate Coating After Various Periods

Time (h)	pH	Ca (μg/mL)	P (μg/mL)	Si (μg/mL)
0	7.42	10	3.1	0
1	7.44	11.17	3.01	0.2
2	7.49	11.17	2.92	0.18
3	7.51	11.91	3.0	0.24
4	7.52	12.18	2.91	0.26
6	7.56	13.15	2.63	0.45
12	7.57	13.73	2.48	0.40
24	7.58	14.35	2.39	0.61
48	7.74	15.6	0.31	0.84

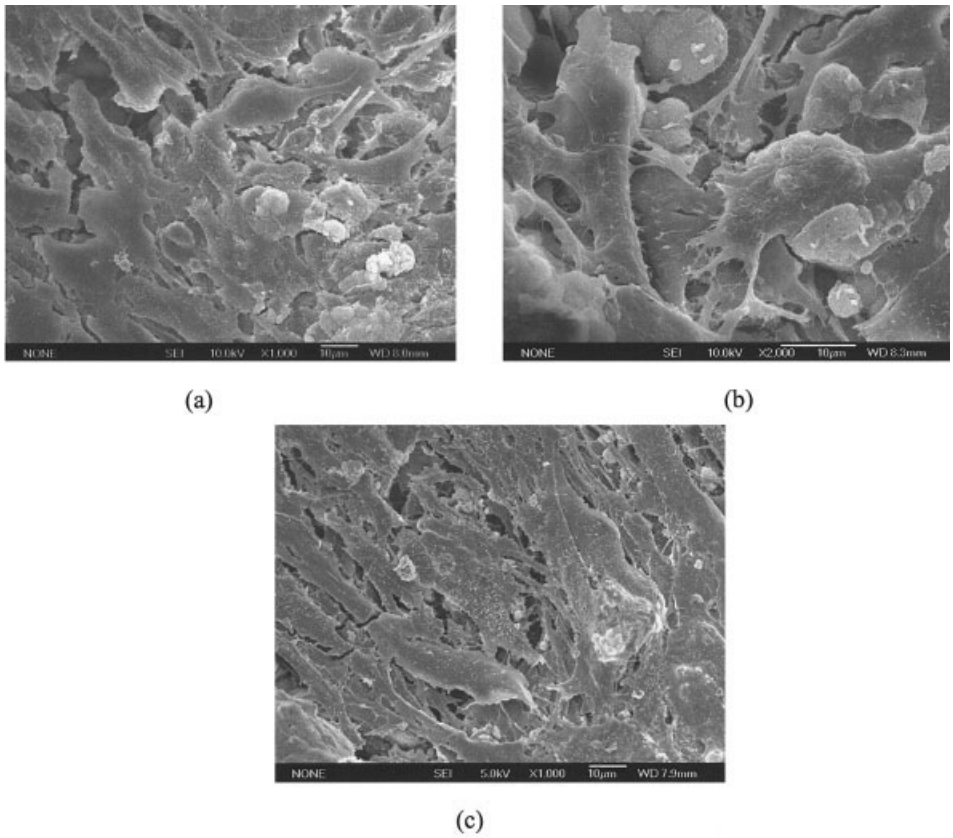

Figure 9. Surface morphologies of the osteoblast-seeded dicalcium silicate coatings after (a) 4 days, (b) 7 days, and (c) 12 days.

tion of the Si 3-ring active surface site with negative charge. The cell-seeding test reveals that osteoblasts grow and proliferate very well on the surface of the dicalcium silicate coating. Therefore, the dicalcium silicate coating possesses excellent bioactivity and biocompatibility.

References

1. Hench LL, Splinter RJ, Allen WC, Greenlee TK. Bonding mechanism at interface of ceramic prosthetic materials. J Biomed Mater Res 1971;2:117–141.
2. Kokubo T. Surface chemistry of bioactive glass-ceramics. J Non-Cryst Solids 1990;120:138–151.
3. Ohtsuki C, Kokubo T, Yamamuro T. Mechanism of apatite formation on CaO-SiO_2-P_2O_5 glasses in a simulated body fluid. J Non-Cryst Solids 1992;143:84–92.
4. De Aza PN, Luklinska ZB, Anseau MR, Hector M, Guitian F, De Aza S. Reactivity of wollastonite-tricalcium phosphate Bioeutectic ceramic in human parotid saliva. Biomaterials 2000;21:1735–1741.
5. Nonami T, Tsutsumi S. Study of diopside ceramics for biomaterials. J Mater Sci Mater Med 1999;10:475–479.
6. Liu X, Ding C. Apatite formed on the surface of plasma sprayed wollastonite coating immersed in simulated body fluid. Biomaterials 2001;22:2007–2012.
7. Liu X, Tao S, Ding C. Bioactivity of plasma sprayed dicalcium silicate coatings. Biomaterials 2002;23:963–968.
8. Kokubo T. A/W glass-ceramic: Processing and properties. In: Hench LL, Wilson J, editors. An introduction to bioceramics. River Edge, NJ: World Scientific; 1993. p 75–88.
9. Hench LL, Anderson O. Bioactive glass. In: Hench LL, Wilson J, editors. An introduction to bioceramics. River Edge, NJ: World Scientific; 1993. p 41–62.
10 Liu X, Ding C, Chu PK. Mechanism of apatite formation on wollastonite coatings in simulated body fluids. Biomaterials 2004;25:1755–1761.
11. Bagambisa FB, Joos U. Preliminary studies on the phenomenological behaviour of osteoblasts cultured on hydroxyapatite ceramics. Biomaterials 1990;11:50–56.
12. Kirkpatrick CJ, Mittermayer C. Theoretical and practical aspects of testing potential biomaterials *in vitro*. J Mater Sci Mater Med 1990;1:9–13.
13. Sahai N, Tossell JA. Molecular orbital study of apatite ($Ca_5(PO_4)_3OH$) nucleation at silica bioceramic surfaces. J Phys Chem B 2000;104:4322–4341.
14. Oliveira JM, Correia RN, Fernandes MH. Effects of Si speciation on the *in vitro* bioactivity of glasses. Biomaterials 2002;23:371–379.
15. Bolt GH. Determination of the charge density of silica sols. J Phys Chem 1957;61:1166–1169.
16. Hildebrand M, Higgins DR, Busser K, Volcani BE. Silicon responsive c-DNA clone isolated from the marine diatom *Cylindrothorax fusiformis*. Gene 1993;132:213.
17. Hench LL. Life and death: The ultimate phase transformation. Thermochim Acta 1996;280/281:1–13.

18. Keeting PE, Wiegand KE, Spelssberg TC, Riggs BL. A novel silicon-containing osteotropic agent, zeolite A, induces proliferation and differentiation of normal human osteoblast-like cells. American Society for Bone and Mineral Research Annual Meeting, Atlanta, GA; Abstract 184.
19. Xynos ID, Hukkanen MVJ, Batten JJ, Buttery ID, Hench LL, Polak JM. Bioglass® 45S5 stimulates osteoblast turnover and enhances bone formation *in vitro*: Implications and applications for bone tissue engineering. Calcif Tissue Int 2000;67:321–329.
20. Xynos ID, Edgar AJ, Buttery LD, Hench LL, Polak JM. Ionic products of bioactive glass dissolution increase proliferation of human osteoblasts and induce insulin-like growth factor II mRNA expression and protein synthesis. Biochem Biophys Res Commun 2000;276:461–465.
21. Vrouwenvelder WCA, Groot CG, de Groot K. Behaviour of fetal rat osteoblasts cultured *in vitro* on bioactive glass and nonreactive glasses. Biomaterials 1992;13: 382–392.